Electronic Supplementary Information

An electrochemical peptide cleavage-based biosensor for prostate specific antigen detection *via* host-guest interaction between ferrocene and β-cyclodextrin

Shunbi Xie[a], Jin Zhang[b,*], Yali Yuan[a], Yaqin Chai[a] and Ruo Yuan[a,*]

[a] Key Laboratory of Luminescent and Real-Time Analytical Chemistry (Southwest University), Ministry of Education, College of Chemistry and Chemical Engineering, Southwest University, Chongqing 400715, PR China

[b] Chongqing Key Laboratory of Environmental Materials & Remediation Technologies (Chongqing University of Arts and Sciences), Chongqing 400715, PR China.

* Corresponding author. Tel.: +86-23-68252277; Fax: +86-23-68253172

E-mail address: zhangjin@cqwu.edu.cn (J. Zhang), yuanruo@swu.edu.cn (R.Yuan)

Experimental Section

Reagents and apparatus

Gold chloride ($HAuCl_4$), bovine serum albumin (BSA), hemoglobin (HB) and ferrocene carboxylic acid (Fc) were purchased from Sigma (St. Louis, MO, USA). α-fetoprotein (AFP), carcino-embryonic antigen (CEA) and prostate specific antigen (PSA) standard solutions were purchased from Biocell (Zhengzhou, China). Carboxylated-Fe_3O_4 (Fe_3O_4-COOH) magnetic microspheres were bought from Tianjin BaseLine ChromTech Research Centre (Tianjin, China). Amine-modified β-cyclodextrin (β-CD) was purchased from Aladdin (Shanghai, China). MWCNTs (>95%

purity) were purchased from Chengdu Organic Chemicals Co. Ltd. of the Chinese Academy of Science. Polyamidoamine (PAMAM) dendrimers were purchased from Weihai CY Dendrimer Technology Co., Ltd (Weihai, China). Tris-hydroxymethylaminomethane hydrochloride (tris) was obtained from Beijing Xiasi Biotechnology Co., Ltd (Beijing, China).

20 mM Tris-HCl buffer (pH 7.4) containing 140 mM NaCl, 5 mM KCl, 1 mM $CaCl_2$ and 1 mM $MgCl_2$ was used as a binding buffer. Phosphate-buffered solution (PBS) (pH 7.4, 0.1 M) containing 10 mM KCl, 2 mM $MgCl_2$ was used as working buffer solution. All other chemicals were of analytical grade and used as received.

All electrochemical measurements, including cyclic voltammetry (CV), differential pulse voltammograms (DPV) were performed on a CHI 660D electrochemical workstation (Shanghai Chenhua Instrument, China). The pH measurements were finished with a pH meter (MP 230, Mettler-Toledo, Switzerland). The scanning electron micrographs were taken with scanning electron microscope (SEM, S-4800, Hitachi). The UV-vis absorption spectra were recorded on a UV-2550 spectrophotometer (Shimadzu, Japan). The structure of nanomaterials was analyzed using Raman spectroscopy (Renishaw InVia Reflex, UK). X-ray diffraction (XRD) was performed with an X-ray diffractometer (Ultima IV, Rigaku, Japan). A three-electrode system contained a modified glassy carbon electrode (GCE, Φ=4 mm) as working electrode, a platinum wire as auxiliary electrode and a saturated calomel electrode (SCE) as reference electrode.

Electrochemical measurements

All electrochemical experiments were carried out in a conventional electrochemical cell containing a three-electrode arrangement. CVs of the electrode fabrication were performed in 2 mL 5 mM $Fe(CN)_6^{3-/4-}$ solution containing 0.2 M KCl,

scanning from -0.6 V to 0.2 V at a scan rate of 100 mV/s. DPV was performed in 2 mL 0.1 M PBS (pH 7.4) to investigate the performance of the sensor. The DPV measurement was taken: the potential range was from 0.1 to 0.7 V, modulation amplitude was 0.05 V, pulse width was 0.05 s, and sample width was 0.0167 s.

Synthesis of Fe_3O_4@Au magnetic nanocomposites

Firstly, gold nanoparticles were prepared according to the reference[1]. Then Fe_3O_4@Au magnetic nanocomposites were synthesized according the reference with some modification[2]. In a typical synthesis, the purified carboxylated-Fe_3O_4 (Fe_3O_4-COOH) magnetic microspheres were functionalized with PDDA. Briefly, 1 mL Fe_3O_4-COOH magnetic microspheres were dispersed into an aqueous solution of 0.2% PDDA (5 mL) containing 20 mM Tris and 20 mM NaCl and sonicated 30 min to obtain a homogeneous black suspension. The generated black precipitate was collected on a magnet and rinsed with water at least three times. Then, 10 mL synthesized gold nanoparticles was mixed with the Fe_3O_4-PDDA precipitate and stored for 1 h. The obtained Fe_3O_4@Au nanocomposite was isolated with magnet and washed several times by ultrapure water. Finally, the Fe_3O_4@Au nanocomposite was dispersed again in 2 mL pH 7.4 PBS and kept at 4 ^{o}C for the following experiment.

Preparation of Fc-peptide conjugate

The conjugate CEHSSKLQLAK-Fc was designed to contain a peptide sequence HSSKLQ, and Fc was conjugated to an N-terminal amino group through a condensation reaction. Its C-terminal is cysteine, whose thiol group is used for coupling to the Fe_3O_4@Au magnetic nanocomposites. The Fc was immobilized on peptide via the interaction between -COOH of Fc and -NH_2 of peptide. The terminal -COOH of Fc were activated by being incubated in the mixture of 40 mM EDC and 10 mM NHS for 2 h at room temperature. And then, the peptide was dissolved in 1 mL

0.1 M activated Fc (pH 5, acetic acid), with a concentration of 50 μM, and stored at -20 °C.

Preparation of the functionalized electrode

First of all, MWCNTs were carboxyl-functionalized and shortened by refluxing in a mixture of concentrated H_2SO_4/HNO_3 (1:3 *v*/*v*) for 40 min at 100 °C, followed by washing to neutrality with ultrapure water[3]. And then, 1 mg carboxyl-functionalized CNTs and 1 mg PAMAM were suspended in 2 mL ultrapure water and sonicated to obtain a homogeneous CNTs-PAMAM black solution, inset of Scheme 1D showed a representative SEM image of CNTs-PAMAM nanohybrids.

Prior to use, the GCE was polished on a polishing cloth with 0.3 and 0.05 mm alumina powder respectively to obtain a mirror-like surface, and sonicated with ethanol and ultrapure water. After that, 10 μL of the CNTs-PAMAM solution was dropped onto the pretreated GCE to increase the effective area of the electrode. Then the electrode was dried at room temperature and immersed in 2.5% glutaraldehyde (GA) solution for 1 h to cross-link amine of the β-CD. Subsequently, 20 μL β-CD (1 mM) was dropped onto the activated platform and incubated for 30 min at room temperature. After each step, the modified electrode was thoroughly cleaned with ultrapure water. The finished functionalized electrode was stored at 4 °C when not used.

Results and discussion

Characterization of the Fc-peptide modified Fe_3O_4@Au biocomplex

The UV-vis absorption spectra were performed to confirm the conjunction of Fe_3O_4@Au/Fc-peptide biocomplex directly. Fig. S1 shows the UV-vis absorbance spectrum for each nanomaterial (AuNPs, Fe_3O_4@Au, and Fe_3O_4@Au/Fc-peptide). AuNPs alone had a singular absorbance peak at 520 nm (curve a), which was red

shifted after the biomaterials were attached to the surface of the Fe_3O_4 and a new absorption band appear at 560 nm, indicating that the successful synthesis of Fe_3O_4@Au (curve d). And the absorption spectra of Fe_3O_4@Au/Fc-peptide complex depending on a new absorption band appeared at 260 nm, which was associated with the Fc-peptide, indicating that the conjunction of the Fc-peptide to Fe_3O_4@Au was successfully synthesized (curve e).

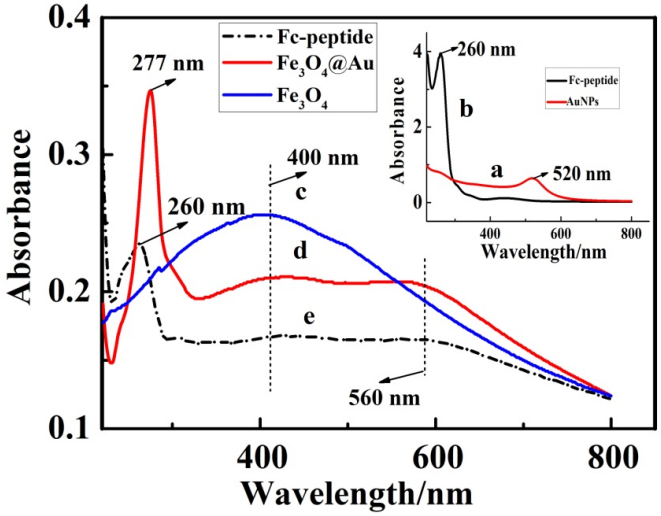

Fig. S1 UV-vis absorption spectra of (a) AuNPs, (b) Fc-peptide, (c) Fe_3O_4-COOH (d) Fe_3O_4@Au (e) Fe_3O_4@Au/Fc-peptide

To further identify the conjunction of Fe_3O_4@Au/Fc-peptide biocomplex, we have performed Raman spectroscopy based on the strong localization of the surface plasmonfield in Fe_3O_4@Au/Fc-peptide biocomplex. The different nanomaterials were casted on a silicon substrate and thus formed aggregates from which the Raman signal was recorded. As shown in Fig. S2, the carboxylated-Fe_3O_4 (Polystyrene magnetic microspheres, purchased from the Tianjin BaseLine ChromTech Research Centre) exhibited four major peaks at 1600, 1311, 1070 and 650 cm^{-1} (curve a). The strong intensity peak at 1002 cm^{-1}, 1311 cm^{-1} and 1601 cm^{-1} were attributable to breathing vibration of the benzene ring, C-O-C stretching and aromatic C=C stretching of polystyrene, respectively. Furthermore, the peak at 650 cm^{-1} was assigned to Fe_3O_4[4].

And the Raman scattering from the surface region of carboxylated-Fe_3O_4 is strongly enhanced after AuNPs coating (curve b), which due to the strong enhancement associated with the intensive surface Plasmon resonance (SPR) of AuNPs. Curve c showed the characteristic peaks of Fc-peptide, the strong intensity peak at 1096 cm^{-1} was attributable to the C-C stretching of Fc[5]. No characteristic peak but silicon substrate (976 cm^{-1}) was observed on the AuNPs (curve e). Curve d displayed the Raman spectra of Fe_3O_4@Au/Fc-peptide biocomplex, it can be seen that the characteristic peaks of Fc (1096 cm^{-1}) and the characteristic peaks of carboxylated-Fe_3O_4 (1600 cm^{-1}), (1311cm^{-1}) and (650 cm^{-1}) were still existed, hence confirming the successfully synthesized of our Fe_3O_4@Au/Fc-peptide biocomplex.

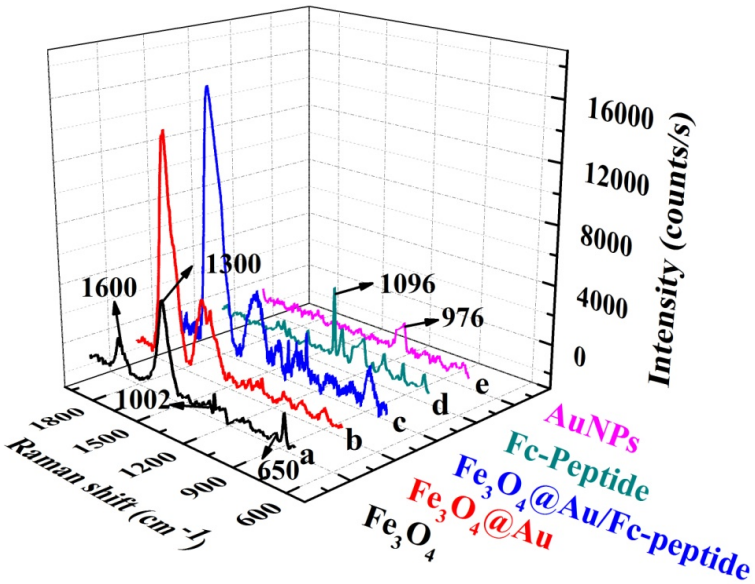

Fig. S2 The Raman spectra of (a) Fe_3O_4-COOH, (b) Fe_3O_4@Au, (c) Fe_3O_4@Au/Fc-peptide and (d) AuNPs.

The X-ray diffraction (XRD) patterns of Fe_3O_4, AuNPs, Fe_3O_4@Au and Fe_3O_4@Au/Fc-peptide were shown in Fig. S3. Curve a showed a typical XRD pattern of the Fe_3O_4 sample, four diffraction peaks at 30.4, 35.6, 57.3 and 62.7 were indexed to the (220), (311), (511) and (440) planes of the Fe_3O_4[6]. As for Fe_3O_4@Au

composites (Curve c), four extra diffraction peaks at 38.2, 44.2, 64.4 and 77.6 (marked as star) were indexed to the (111), (200), (220) and (311) planes of the Au cubic phase[7], which is the same as typical XRD pattern of AuNPs (curve b). Curve d is a typical XRD pattern of the Fe_3O_4@Au/Fc-peptide, which shows almost the same feature as that shown in curve c: no diffraction peaks corresponding to Fc-peptide were observed because the prepared Fc-peptide is biomolecule.

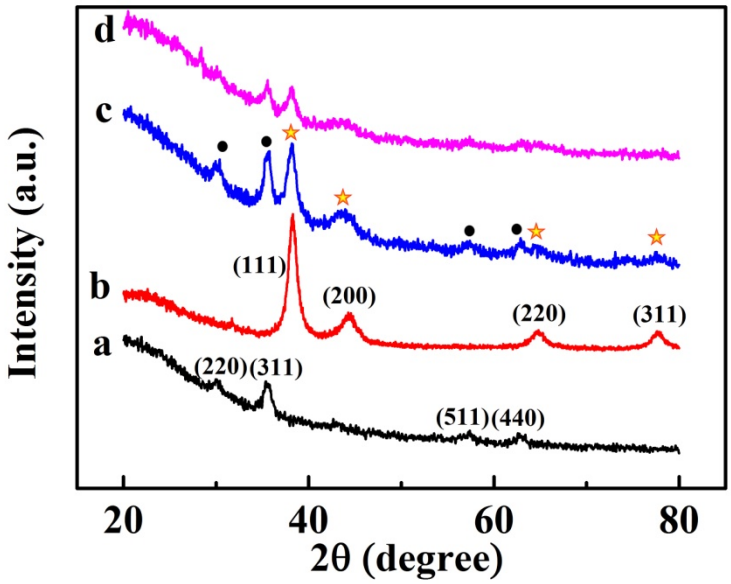

Fig. S3 X-ray diffraction patterns of (a) Fe_3O_4-COOH, (b) AuNPs, (c) Fe_3O_4@Au and (d) Fe_3O_4@Au/Fc-peptide.

The electroactive surface area of the CNTs-PAMAM modified electrode

In order to illustrate that the prepared CNTs-PAMAM nanohybrids could improve the surface area and conductivity of the biosensor, we designed an experiment to quantitatively detect the electro-active surface area of CNTs-PAMAM modified electrode by recording CVs at different potential scan rates with $Fe(CN)_6^{4-/3-}$ serving as redox probes. From Fig. S4 A and Fig. S4 B, we could see that the redox peak currents were proportional to the square root of scan rates in the

range of 20-300 mVs^{-1} with the regression equation of $I = 931.6\ v^{1/2} - 31.12$ (anodic peak current) and $I = -892.4\ v^{1/2} + 24.64$ (cathodic peak current). The calculated electro-active surface area was 26.12 mm^2 according to the Randles-Sevcik equation[8,9] $I = 2.69\times10^5 A\times D^{1/2} n^{3/2} v^{1/2} C$, in which n is the number of electrons transferred in the redox reaction (n= 1), A is the electrode area, D is the diffusion coefficient (at 25 °C, D=6.70×10^{-6} cm^2s^{-1}), C is the concentration of the reactant (5.0 mol cm^{-3} $Fe(CN)_6^{3-/4-}$), I refers to the redox peak current and v is the scan rate of the CV measurement.

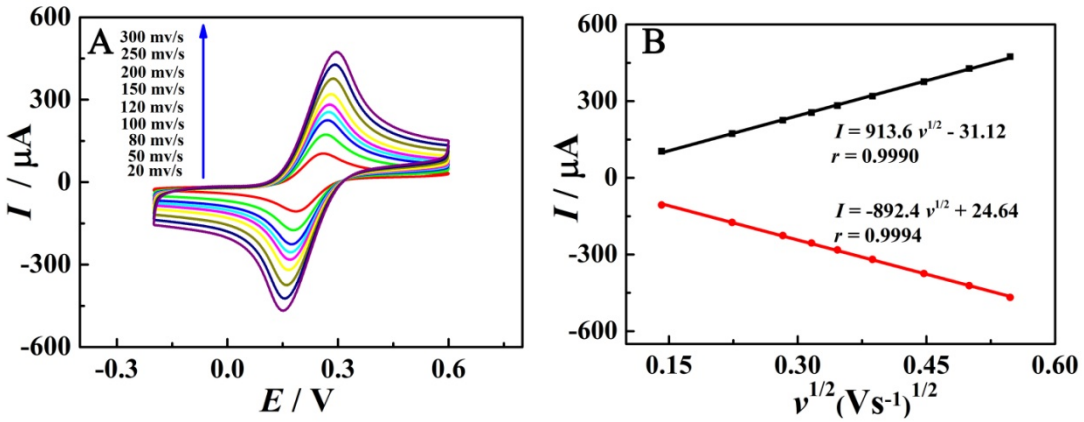

Fig. S4 CVs of CNTs-PAMAM modified GCE in 5.0 mM $Fe(CN)_6^{4-/3-}$ at different scan rates from 20 to 300 mV s-1 (A). The linear relations of the CNTs-PAMAM modified GCE with the anodic and cathodic peak current against the square root of scan rate (B).

The inclusion of the surface-attached Fc on the GCE/CNTs-PAMAM/β-CD functionalized electrode

In order to investigate the inclusion of the surface-attached Fc on the GCE/CNTs-PAMAM/β-CD functionalized electrode, we performed cyclic voltammetry at GCE/CNTs-PAMAM/β-CD functionalized electrode incubated increasing Fc concentrations (Fig. S5). As we can see from Fig. S5 A, the cathodic peak currents increased with the increasing concentration of Fc, and eventually

reached a steady value at concentrations above 80 μM. And the dose response curve showed a strong linear dependence of current on Fc concentrations in the range from 10 μM to 70 μM with the regression equation of I = -0.101 c -3.2913 (Fig. S5 B). We can estimate the maximum amount of Fc on the electrode surface through above regression equation. The calculated maximum amount of Fc on the electrode surface was 63.6 μM.

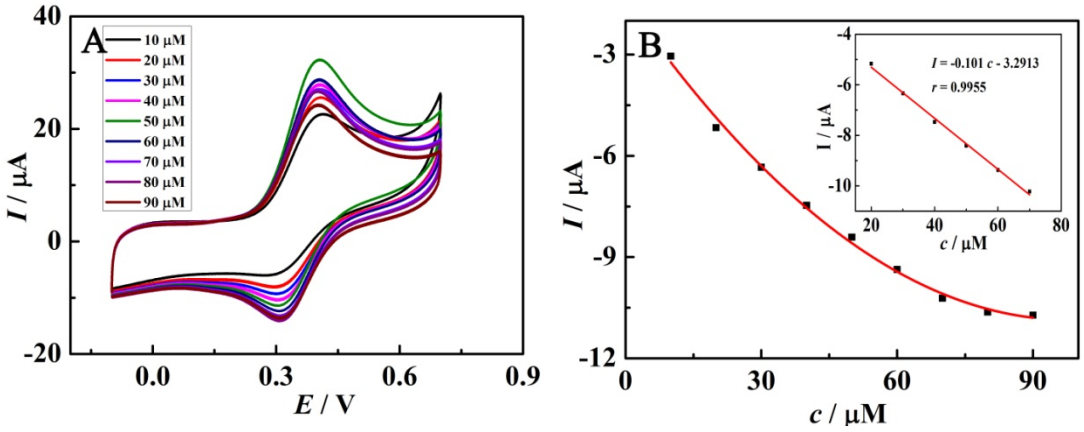

Fig. S5 Cyclic voltammograms, recorded at GCE/CNTs-PAMAM/β-CD functionalized electrode incubating with different concentration of Fc (from 10 μM to 90 μM) in 2 mL PBS (pH 7.4), Scan rate: 100 mV/s (A); The dependence of peak currents on each concentration of Fc, the insert showed the calibration plot of current intensity *vs* c_{Fc} (B).

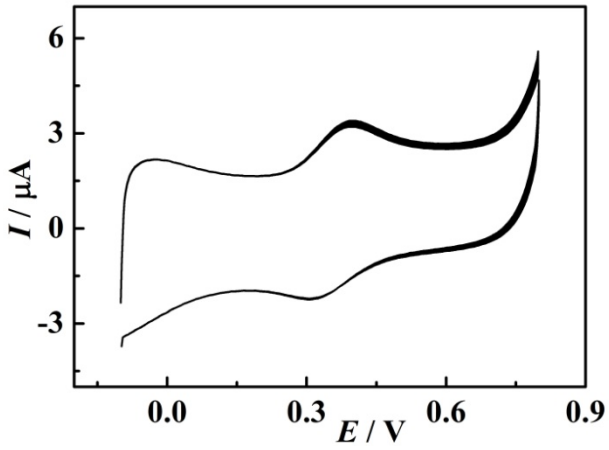

Fig. S6 Stability of the proposed biosensor incubated with 0.05 ng/mL PSA under successive CV scans for 50 cycles.

Table S1. The proposed method compared with other PSA analytical performance.

Analytical method	Detection limit	Linear range	Ref.
SWV	0.2 ng/mL	0.5-40 ng/mL	10
SWV	2 pg/mL	0.01-40 ng/mL	11
DPV	0.02 ng/mL	0.2-40 ng/mL	12
CV	0.015 ng/mL	0.05-50 ng/mL	13
Potentiometry	2.6 ng/mL	3.5-30 ng/mL	14
ECL	8 pg/mL	0.01-8 ng/mL	15
DPV	0.78 pg/mL	0.001-30 ng/mL	This work

Abbreviation: Square-wave voltammograms (SWV); Differential pulse voltammetry (DPV); Cyclic voltammetry (CV); Electrochemiluminescent (ECL).

Table S2. Determination of PSA added in human blood serum (*n=3*) with the proposed sensor

Sample No.	Amount of PSA added to the serum/(ng/mL)	Amount of PSA detected by the sensor/(ng/mL)	Recovery/%	RSD/%
1	1	1.057	105.7	4.32
2	10	10.12	101.2	5.45
3	20	20.5	102.5	3.78
4	30	31.89	106.3	6.57

References

1. G. Frens, Nature-Phys. Sci., 1973, 241, 20-22.
2. D. Du, Y. Tao, W. Y. Zhang, D. L. Liu and H. B. Li, Biosens. Bioelectron., 2011, 26, 4231-4235.
3. X. Yang, R. Yuan, Y. Q. Chai, Y. Zhuo, L. Mao and S. R. Yuan, Biosens. Bioelectron, 2010, 25, 1851-1855.
4. A. Mezni, I. Balti, A. Mlayah, N. Jouini and Leila Samia Smiri, J. Phys. Chem. C., 2013, 117, 16166-16174.
5. Y. Chen, A. Klimczak, E. Galoppini and J. V. Lockard, RSC Adv., 2013, 3, 1354-1358.
6. X. Zhou, W. L. Xu, Y. Wang, Q. Kuang, Y. F. Shi, L. B. Zhong and Q.Q. Zhang, J. Phys. Chem. C, 2010, 114, 19607-19613.
7. Q. J. Du, L.F. Tan, Bo. Li, T.L. Liu, J. Ren, Z.B. Huang, F.Q. Tang and X.W. Meng, RSC Adv., 2014, 4, 56057-56062.

8. A. J. Bard and L. R. Faulkner, Electrochemical Methods Fundamentals and Applications; John Wiley & Son: New York, 1980.
9. P. Zanello, "Inorganic Electrochemistry: Theory, Practice and Application" The Royal Society of Chemistry 200.
10. N. Zhao, Y. Q. He, X. Mao, Y. H. Sun, X. B. Zhang, C. Z. Li, Y. H. Lin and G. D. Liu, Electrochem. Commun., 2010, 12, 471-474.
11. H. Li, Q. Wei, J. He, T. Li, Y. F. Zhao, Y. Y. Cai, B. Du, Z. Y. Qian and M. H. Yang, Biosens. Bioelectron., 2011, 26, 3590-3595.
12. A. Salimi, B. Kavosi, F. Fathi and R. Hallaj, Biosens. Bioelectron., 2013, 42, 439-446.
13. H. Wang, Y. Zhang, H. Yu, D. Wu, H. Ma, H. Li, B. Du and Q. Wei, Anal. Biochem., 2013, 434, 123-127.
14. G. Shen, C. Cai and J. Yang, Electrochim. Acta., 2011, 56, 8272-8277.
15. S. J. Xu, Y. Liu, T. H. Wang and J. H. Li, Anal. Chem., 2011. 83, 3817-3823.